



*Supplement of*

## **Model simulations of arctic biogeochemistry and permafrost extent are highly sensitive to the implemented snow scheme in LPJ-GUESS**

**Alexandra Pongracz et al.**

*Correspondence to:* Alexandra Pongracz (alexandra.pongracz@nateko.lu.se)

The copyright of individual parts of the supplement might differ from the article licence.

## S1 Adjusted respiration rate

We defined a new function following Natali et al. (2019), shown in Fig S1. The Q<sub>10</sub> value was changed from the previous value of 200.5 to 2.9. Additionally, the minimum temperature threshold was set to -20 °C instead of the previously used -4 °C.

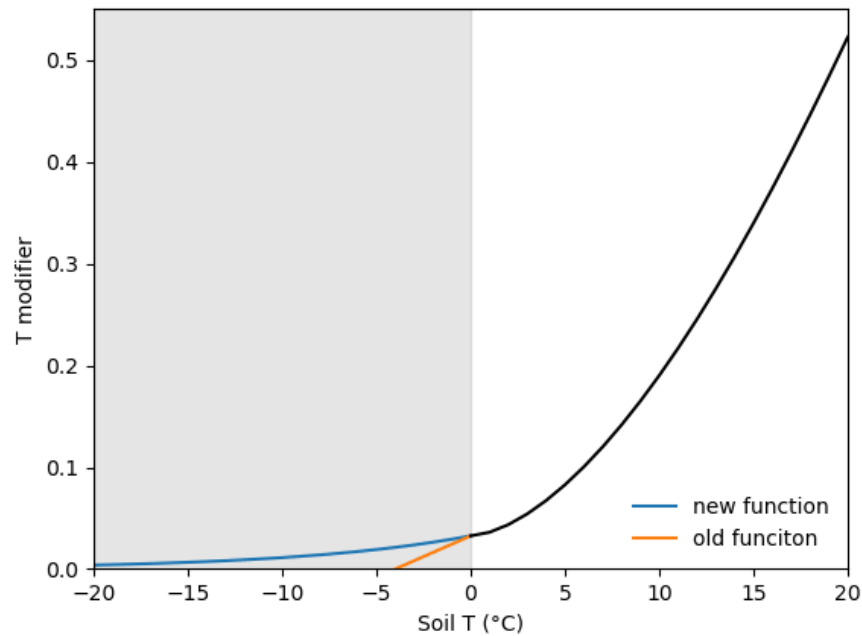


**Figure S1:** The old and new function controlling respiration rate during cold conditions.

## S2 Site simulation details

Years of observational data used for the site simulations on Abisko, Bayelva, Kytalyk, Samoylov and Zackenberg sites (PAGE21 sites) can be seen in Table S1. The computed RMSE between observed and modelled near surface soil temperature and air-soil temperature difference is shown in Table S2.

**Table S1:** Snow depth and near surface soil temperature data used for the site simulations, and climatic zones of the sites. (Sect.3.1)

	latitude	longitude	snow depth	soil T	climatic zone	reference
Abisko	68.35	19.05	1986-2020	2021-2015	sub-arctic	Johansson et al. (2011, 2013)
Bayelva	78.92	11.93	1998-2009	1998-2017	high-arctic	Boike et al. (2017)
Kytalyk	70.83	147.5	2011-2013	2004-2011	low-arctic	Parmentier et al. (2011)
Samoylov	72.22	126.28	1996-2013	2012-2014	low-arctic	Boike et al. (2018)
Zackenberg	74.5	-20.6	1996-2011	1995-2017	high-arctic	Greenland Ecosystem Monitoring (2020)

**Table S2:** RMSE for soil temperature and  $\Delta T$  for the applied snow schemes, and temperature regimes at the Russian sites (Sect. 3.2).

		RMSE (°C)		
		-15 °C < $T_{air}$ < -5 °C	-25 °C < $T_{air}$ < -15 °C	$T_{air} < -25$ °C
Soil T (°C)		Static	Dynamic	
	Static	6.36	0.86	12.18 1.1
	Dynamic			17.87 2.9
$\Delta T$ (°C)	Static	6.98	1.32	12.29 0.78
	Dynamic			19.28 3.78

## S3 Pan-Arctic simulations

### S3.1 Simulated physical variables

These figures show the spatial pattern of simulated variables averaged over 1990-2015. Summer season values are averaged over June, July and August and winter season values are averaged over December, January and February.

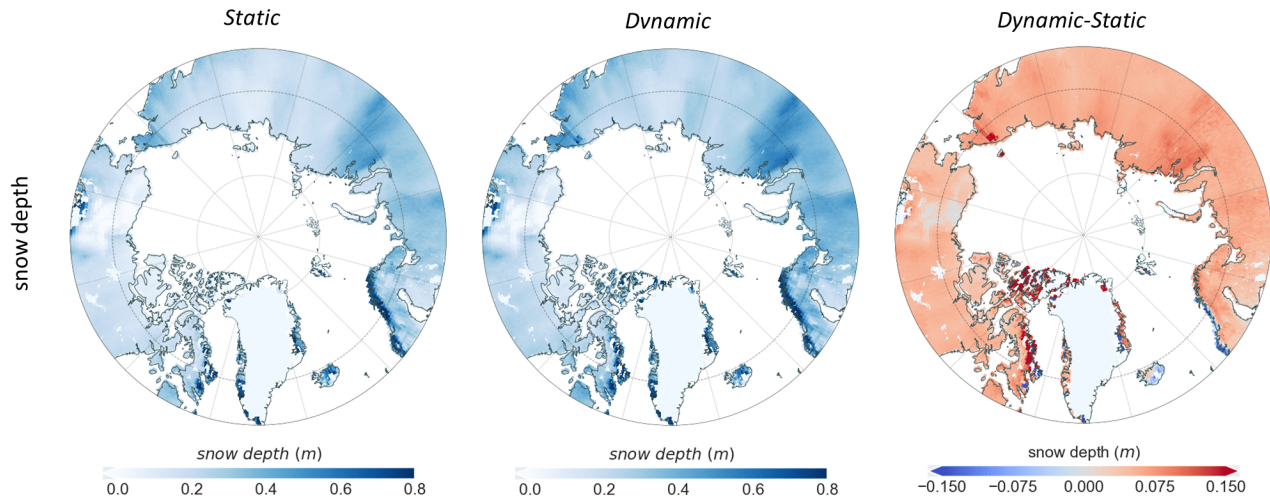


**Figure S2:** Simulated snow depth using the *Static* and *Dynamic* snow schemes and their difference.

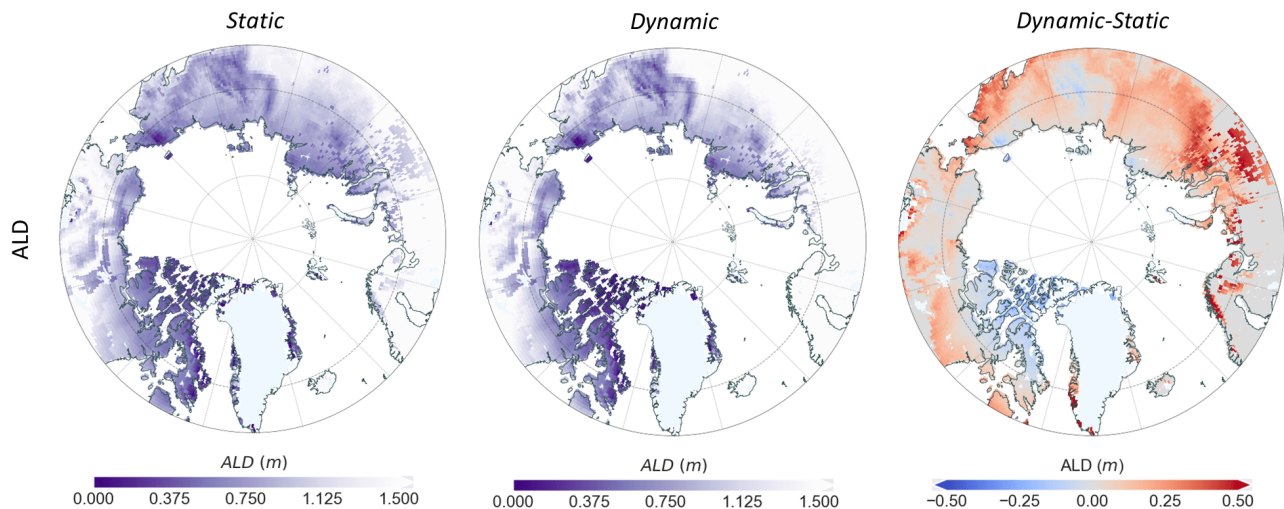


**Figure S3:** Simulated maximum annual active layer depth (ALD) using the *Static* and *Dynamic* snow schemes and their difference.

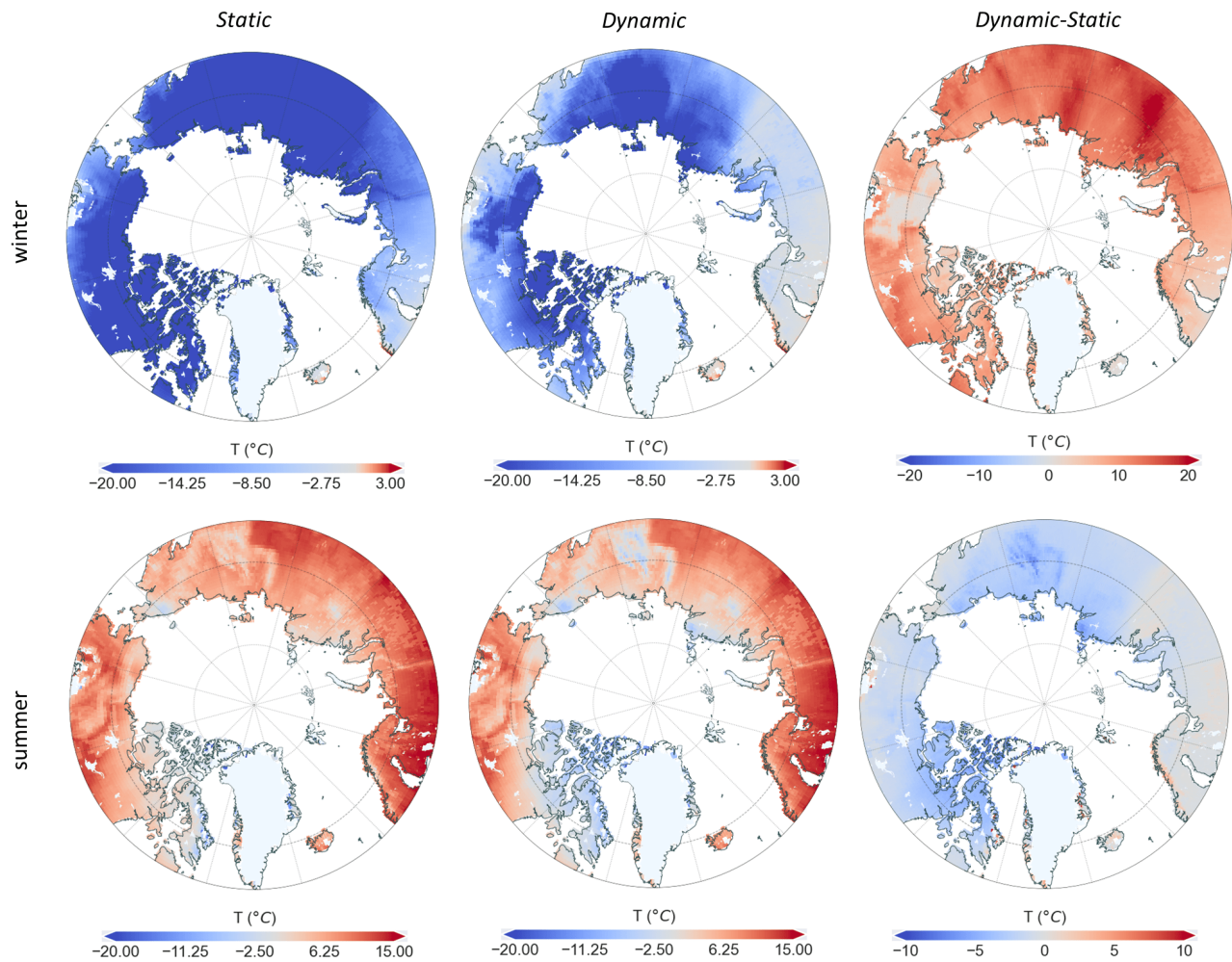


**Figure S4:** Simulated near surface soil temperature (25 cm depth) using the *Static* and *Dynamic* snow schemes and their difference for winter and summer.

### S3.2 Simulated biogeochemical variables

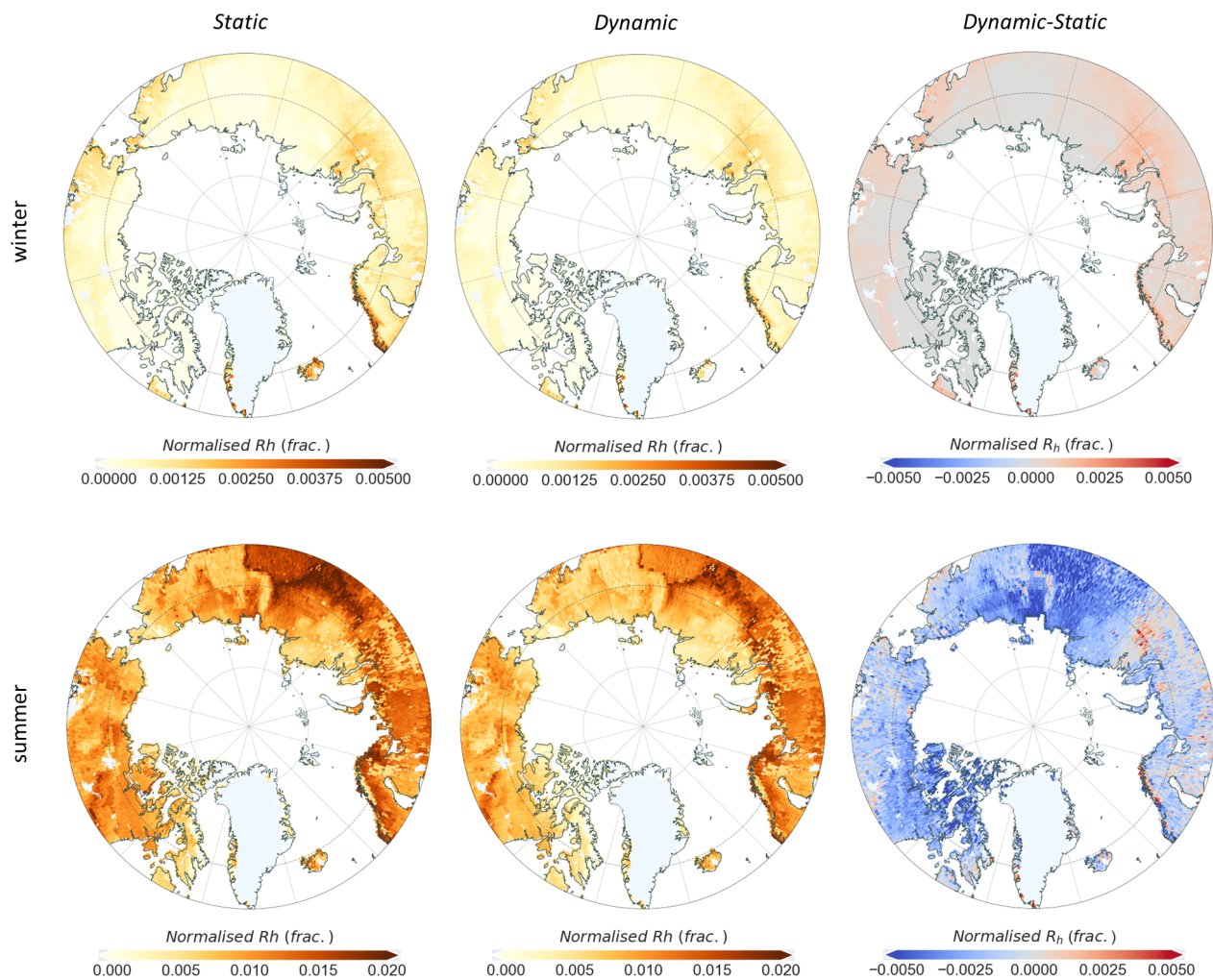


**Figure S5:** Simulated heterotrophic respiration normalised by soil carbon content, using the *Static* and *Dynamic* snow schemes and their difference for winter and summer.

### S3.3 Simulated biogeochemical variables

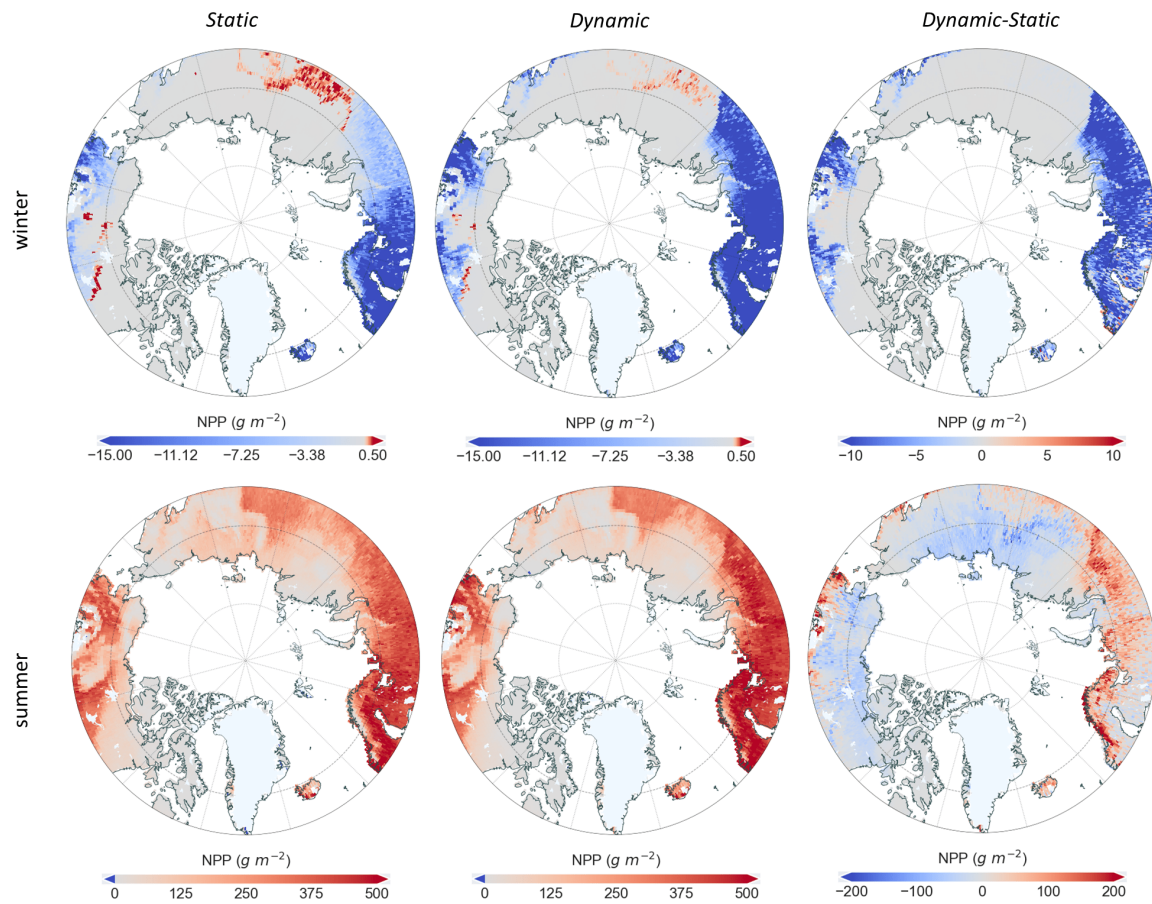


**Figure S6:** Simulated NPP using the *Static* and *Dynamic* snow schemes and their difference for winter and summer.

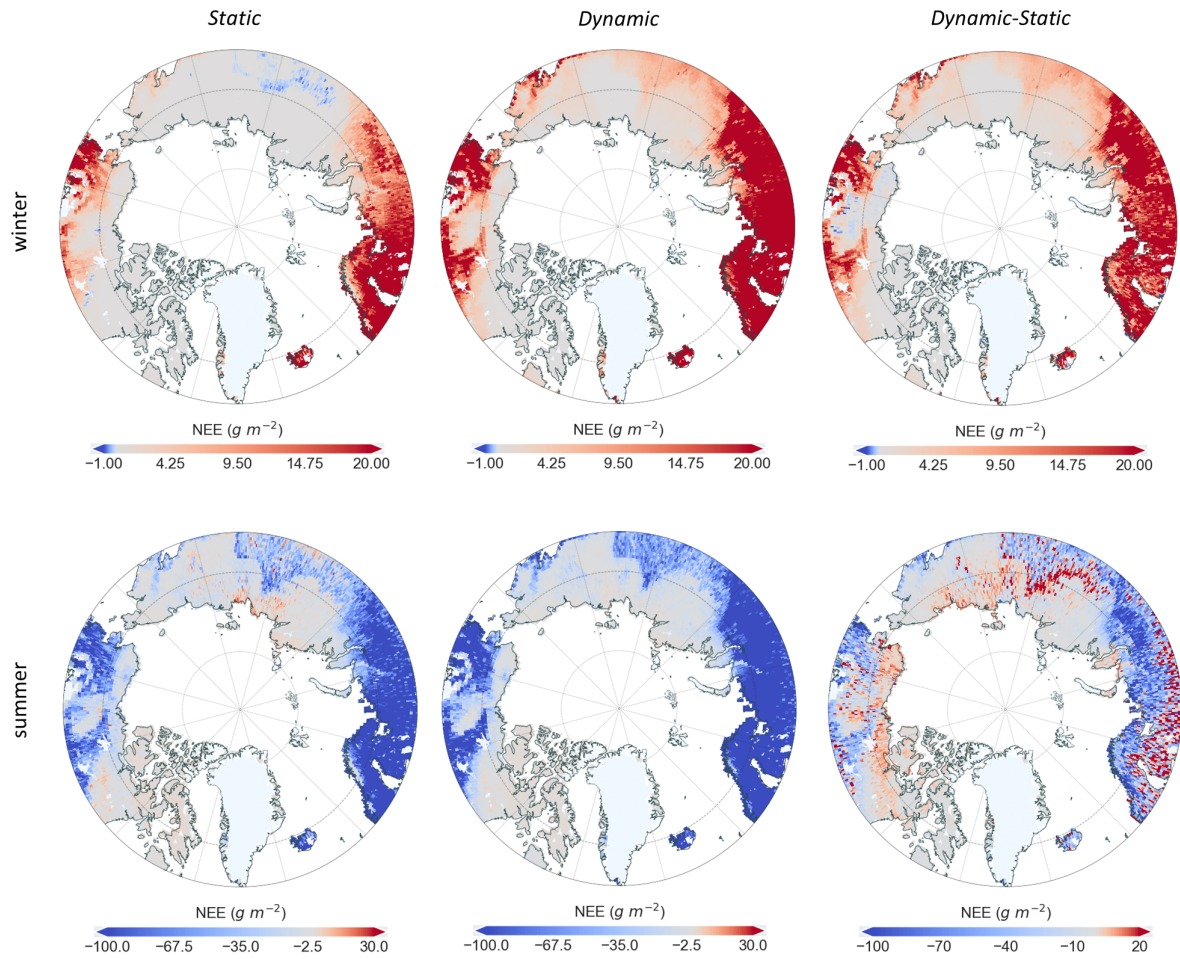


**Figure S7:** Simulated NEE using the *Static* and *Dynamic* snow schemes and their difference for winter and summer.

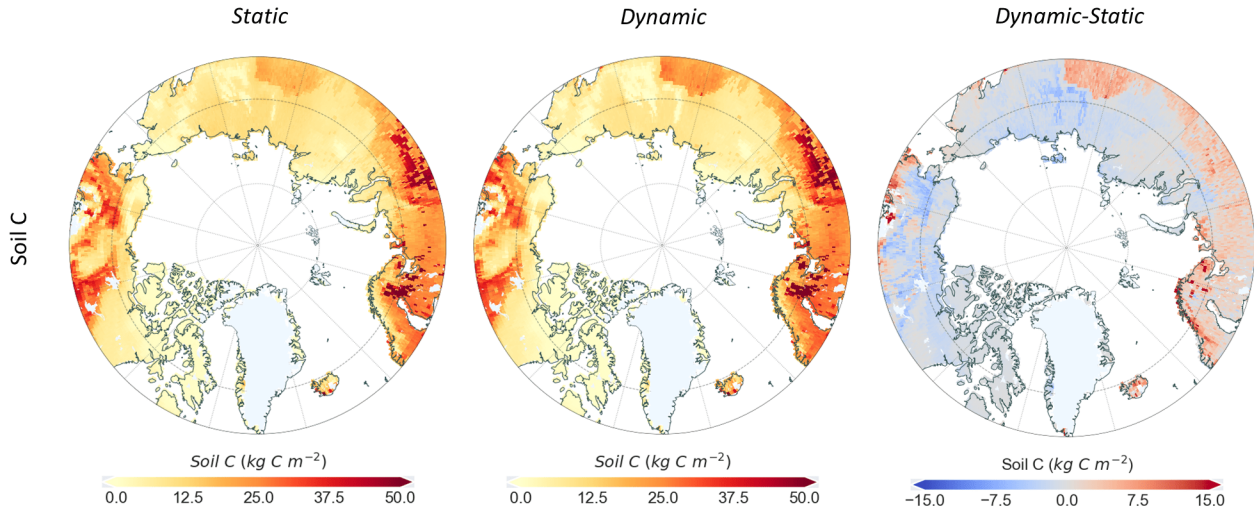


**Figure S8:** Simulated soil carbon content, using the *Static* and *Dynamic* snow schemes and their difference for winter and summer.

### S3.4 Nitrogen cycling

Besides the carbon-related fluxes, we also assessed the impact of snow on nitrogen cycling. Figure S9 shows the nitrogen mineralisation (Fig. S9 (a)) and leaching (Fig. S9 (b)) normalised by soil carbon content. Nitrogen mineralisation only changed markedly during the summer season within the permafrost region. Leaching is higher for the *Dynamic* scheme in Eastern-Canada and Northern-Russia. Nitrogen use efficiency (NUE) on panel (c) was calculated as the ratio between NPP and nitrogen uptake. The *Dynamic* scheme simulates a lower NUE than the *Static* scheme, which indicates a higher N uptake per unit productivity.

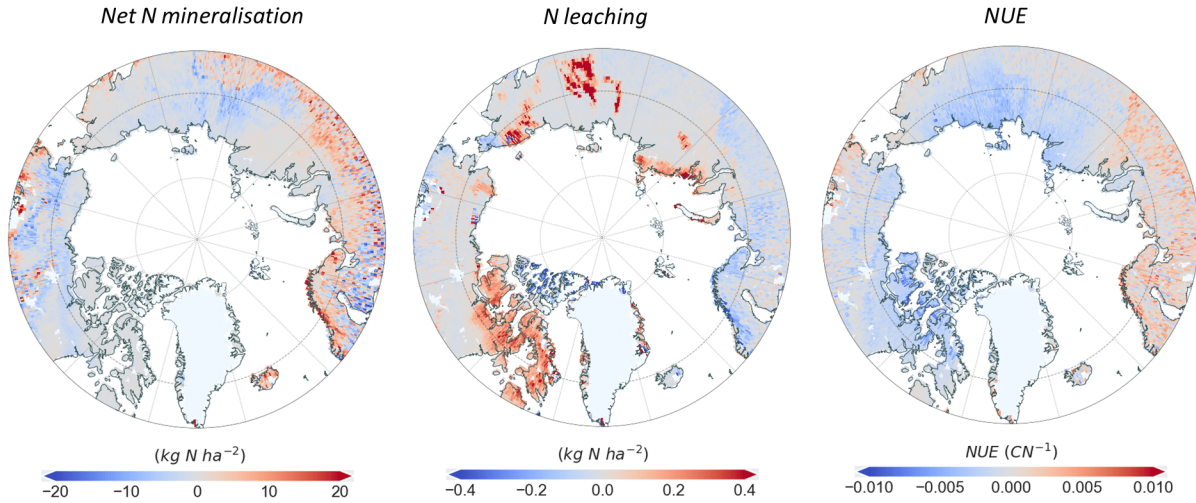


**Figure S9:** Nitrogen mineralisation, N leaching and NUE difference calculated by subtracting the *Static* from *Dynamic* simulation outputs.

### S3.5 Vegetation dynamics

**Table S3:** Applied PFTs and vegetation grouping, based on Wolf et al. (2008)

PFT	Description	Vegetation group
BNE	Boreal needleleaved evergreen tree	forest
BINE	Boreal needleleaved evergreen tree	forest
BNS	Boreal needleleaved summergreen tree	forest
IBS	Shade-intolerant broadleaved summergreen tree	forest
TeBS	Shade-tolerant temperate broadleaved summergreen tree	forest
HSE	Tall shrub, evergreen	shrub
HSS	Tall shrub, summergreen	shrub
LSE	Low shrub, evergreen	shrub
LSS	Low shrub, summergreen	shrub
GRT	Graminoid and forb tundra	grass
EPDS	Prostrate dwarf shrubs (needleleaved, evergreen)	grass
SPDS	Prostrate dwarf shrubs (broadleaved, summergreen)	grass
CLM	Cushion forb, lichen and moss tundra	grass
C3G	C3 grass	grass

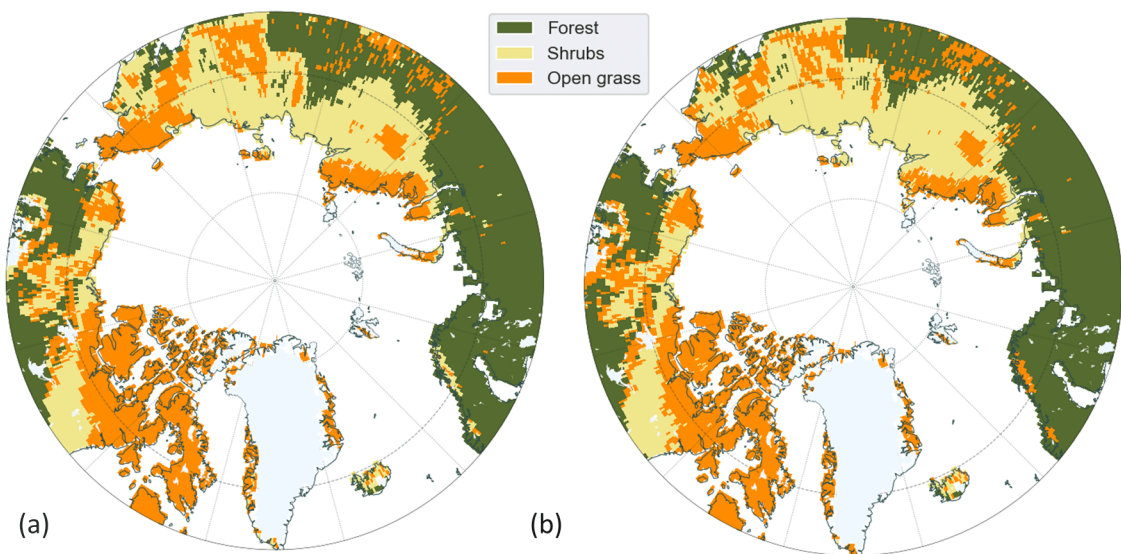


**Figure S10:** Vegetation distribution for the *Static* (a) and *Dynamic* schemes (b).

Sites where PFT dominance changed between the *Static* and *Dynamic* simulations is shown in Fig. S11. These transition sites are scattered across the Arctic, but there are some clear hotspots in Eastern-Russia, the Scandinavian coastline and Northern-America.

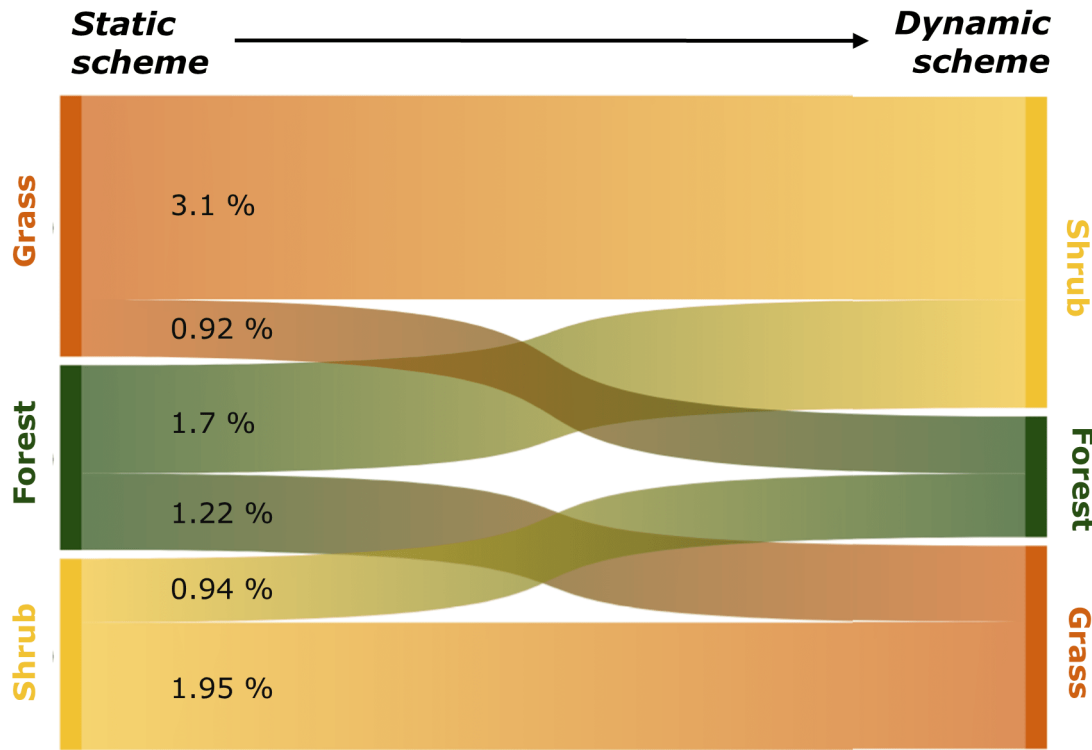


**Figure S11:** Direction of dominant vegetation group changes between the *Static* and *Dynamic* schemes. The size of arrows are proportional to the number of sites transitioning. The percentages on arrows show the portion of total simulated sites.

## References

Boike, J., Juszak, I., Lange, S., Chadburn, S., Burke, E. J., Overduin, P. P., Roth, K., Ippisch, O., Bornemann, N., Stern, L., Gouttevin, I., Hauber, E. & Westermann, S. (2017), ‘Measurements in soil and air at Bayelva Station’. Supplement to: Boike, J et al. (2018): A 20-year record (1998–2017) of permafrost, active layer and meteorological conditions at a high Arctic permafrost research site (Bayelva, Spitsbergen). Earth System Science Data, 10(1), 355–390, <https://doi.org/10.5194/essd-10-355-2018>.

**URL:** <https://doi.org/10.1594/PANGAEA.880120>

Boike, J., Nitzbon, J., Anders, K., Grigoriev, M. N., Bolshiyanov, D. Y., Langer, M., Lange, S., Bornemann, N., Morgenstern, A., Schreiber, P., Wille, C., Chadburn, S., Gouttevin, I. & Kutzbach, L. (2018), ‘Measurements in soil and air at Samoylov Station (2002–2018)’. Supplement to: Boike, Julia; Nitzbon, Jan; Anders, Katharina; Grigoriev, Mikhail N; Bolshiyanov, Dmitry Yu; Langer, Moritz; Lange, Stephan; Bornemann, Niko; Morgenstern, Anne; Schreiber, Peter; Wille, Christian; Chadburn, Sarah; Gouttevin, Isabelle; Burke, Eleanor J; Kutzbach, Lars (2019): A 16-year record (2002–2017) of permafrost, active-layer, and meteorological conditions at the Samoylov Island Arctic permafrost research site, Lena River delta, northern Siberia: an opportunity to validate remote-sensing data and land surface, snow, and permafrost models. Earth System Science Data, 11(1), 261–299, <https://doi.org/10.5194/essd-11-261-2019>.

**URL:** <https://doi.org/10.1594/PANGAEA.891142>

Greenland Ecosystem Monitoring (2020), ‘Geobasis zackenberg - flux monitoring - ac’.

**URL:** <https://data.g-e-m.dk/datasets?doi=10.17897/430P-DS31>

Johansson, Cecilia, ., Pohjola, Veijo A., ., Jonasson, C. & Callaghan, T. (2011), ‘Multi-decadal changes in snow characteristics in sub-arctic sweden.’, *Ambio* 40(6), 566 – 574.

Johansson, M., Callaghan, T. V., Bosiö, J., Åkerman, J., Jackowicz-Korczynski, M. & Christensen, T. (2013), 'Rapid responses of permafrost and vegetation to experimentally increased snow cover in sub-arctic sweden.', *Environmental Research Letters* **8**(3).

Natali, S. M., Watts, J. D., Rogers, B. M., Potter, S., Ludwig, S. M., Selbmann, A.-K., Sullivan, P. F., Abbott, B. W., Arndt, K. A., Birch, L., Bjorkman, M. P., Bloom, A. A., Celis, G., Christensen, T. R., Christiansen, C. T., Commande, R., Cooper, E. J., Crill, P., Czimczik, C., Davydov, S., Du, J., Egan, J. E., Elberling, B., Euskirchen, E. S., Friberg, T., Genet, H., Göckede, M., Goodrich, J. P., Grogan, P., Helbig, M., Jafarov, E. E., Jastrow, J. D., Kalhorni, A. A. M., Kim, Y., Kimball, J. S., Kutzbach, L., Lara, M. J., Larsen, K. S., Lee, B.-Y., Liu, Z., Loranty, M. M., Lund, M., Lupascu, M., Madani, N., Malhotra, A., Matamala, R., McFarland, J., McGuire, A. D., Michelsen, A., Minions, C., Oechel, W. C., Olefeldt, D., Parmentier, F.-J. W., Pirk, N., Poulter, B., Quinton, W., Rezanezhad, F., Risk, D., Sachs, T., Schaefer, K., Schmidt, N. M., Schuur, E. A. G., Semenchuk, P. R., Shaver, G., Sonnentag, O., Starr, G., Treat, C. C., Waldrop, M. P., Wang, Y., Welker, J., Wille, C., Xu, X., Zhang, Z., Zhuang, Q. & Zona, D. (2019), 'Large loss of co<sub>2</sub> in winter observed across the northern permafrost region', *Nature Climate Change* **9**(11).

Parmentier, F. J. W., van der Molen, M. K., van Huissteden, J., Karsanaev, S. A., Kononov, A. V., Suzdalov, D. A., Maximov, T. C. & Dolman, A. J. (2011), 'Longer growing seasons do not increase net carbon uptake in the northeastern siberian tundra', *Journal of Geophysical Research: Biogeosciences* **116**(G4).

**URL:** <https://agupubs.onlinelibrary.wiley.com/doi/abs/10.1029/2011JC001653>

Wolf, A., Callaghan, T. V. & Larson, K. (2008), 'Future changes in vegetation and ecosystem function of the barents region.', *Climatic Change* **87**(1-2), 51 – 73.